Energy exchange in neutrino nuclear scattering

V. N. Kondratyev,[1,2,*] Alan A. Dzhioev,[1] A. I. Vdovin,[1] S. Cherubini,[3] and M. Baldo[3]
[1]*Bogoliubov Laboratory of Theoretical Physics, JINR, 141980 Dubna, Russia*
[2]*Department of Physics, Dubna State University, 141982 Dubna, Russia*
[3]*Department of Physics and Astronomy "Ettore Majorana", University of Catania, Catania 95123, Italy*

(Received 15 June 2019; published 9 October 2019)

Neutrino nuclear scattering in hot and dense matter relevant for supernovae, neutron star mergers, and proto-neutron stars is considered. At finite temperature, neutrinos exhibit exo- and endoenergetic scattering on nuclear species due to the neutral-current Gamow-Teller interaction component. From an analysis of energy transfer and straggling cross sections we demonstrate that additional noticeable mechanisms in equilibrating neutrinos with matter originate in magnetized nucleon gas. Average energy transfer, i.e., ratio of energy transfer and scattering cross sections, depends almost linearly on neutrino energy and changes from positive to negative value. For hot nuclear material such crossover between acceleration and stopping regimes occurs when neutrino energy is about a factor four of temperature. Similar features are displayed for neutrino scattering on hot atomic nuclei. For the ^{56}Fe nucleus the stopping regime starts at energies slightly above than four times temperature. Possible effects in neutrino transport and spectra are discussed.

DOI: 10.1103/PhysRevC.100.045802

I. INTRODUCTION

Interaction of neutrinos with matter represents an important issue in various astrophysical phenomena, e.g., core-collapse supernovae, neutron star mergers, formation of neutron star crusts, etc. In particular, neutrino flux and/or magnetic pressures are considered as an additional key contribution to supernova (SN) explosive shock wave formation and a possible mechanism of energy transfer to all initially bound matter of the progenitor star. In a delayed (neutrino heating) explosion scenario the stalled shock wave can be revived by electron neutrinos and antineutrinos radiated by a cooling proto-neutron star [1,2]. Neutrino absorption on nucleons results in an increase of the internal energy and pressure of the matter behind the shock, which starts to expand, pushing the shock forward. The efficiency of such a delayed SN mechanism depends on neutrino luminosity and a hardness of their spectra [2].

In addition, multidimensional effects like convection and plasma instabilities can contribute to successful explosions, as suggested by modern supernova simulations [3–12]. The violent convection bringing magnetorotational instabilities (MRI) and/or dynamo-action processes can result in enormous magnetic induction amplification with extremely large field strengths up to tens of *teratesla* (TT). The corresponding magnetic pressure pumps energy to the star material and can be considered as a predominant mechanism of shock wave formation for prompt explosion scenarios. Pioneering observational evidence in support of ultramagnetized astrophysical objects ("magnetars") is associated with the discovery [13] of the famous 5 March 1979 event of a super intense gamma-ray outburst (giant flare) from SGR 0526-66.

Neutrino and/or magnetic pressures contributing significantly to SN explosions requires urgent analysis of neutrino transport in the SN environment to account for magnetic effects. It was first pointed by Haxton [14] that neutral- and charged-current neutrino reactions on nuclei can play an important role in SN explosions. Incorporation of such reactions into core-collapse simulations [15,16] has shown that the inelastic neutrino scattering on nuclei is of the same importance as the neutrino-electron scattering in equilibrating neutrinos with matter. In this work we analyze effect of the baryonic component for neutrino transport in hot and dense matter. As is demonstrated, additional inelastic neutrino nuclear reaction channels arise in the magnetized SN environment. Such channels induced by magnetic field are shown to give an effect similar to that of scattering on nuclei.

II. NEUTRINO TRANSPORT IN STELLAR MATTER

For a quantitative description of energy transfer at neutrino scattering on nuclear species of hot supernova matter we consider energy weighted integral values

$$S_n(E_\nu, T) = \frac{G_F^2}{\pi} g_A^2 \int_{-\infty}^{E_\nu} (-E)^n (E_\nu - E)^2 \Sigma_{\mathrm{GT}_0}(E, T)\, dE, \tag{1}$$

where G_F is the Fermi weak interaction constant and $g_A = -1.26$ gives the axial-vector coupling constant. The value of S_0 represents the cross section, S_1 gives average energy transfer (i.e., stopping) cross section between the neutrino and the nuclear system, and S_2 corresponds to the energy straggling. In the thermal strength function $\Sigma_{\mathrm{GT}_0}(E;T)$ we include only the contribution of the charge-neutral

*vkondrat@theor.jinr.ru

Gamow-Teller (GT) operator $\mathrm{GT}_0 = \boldsymbol{\sigma} t_0$:

$$\Sigma_{\mathrm{GT}}(E;T) = Z^{-1}(T) \sum_{i,f} e^{-E_i/T} \langle i|\mathrm{GT}_0|f\rangle|^2 \delta(E - E_{fi}), \quad (2)$$

where $Z(T)$ is the nucleon or nuclear partition function, $\boldsymbol{\sigma}$ denotes the spin operator, while t_0 is the zero component of the isospin operator. The definition of $\Sigma_{\mathrm{GT}}(E;T)$ implies that the transition energy $E_{fi} = E_f - E_i$ can be both positive and negative corresponding to endo- and exoenergetic neutrino scattering.

A. Neutrino scattering in magnetized nondegenerate nucleon gas

Neutrino scattering in nucleon gas, $\nu + N \to \nu' + N'$, represents the simplest relevant problem. This case yields transparent and clear results for cross sections, rates, energy transfer, and straggling with fundamental consequences for neutrino dynamics in hot nuclear matter at strong magnetic fields. The SN matter close to and behind the neutrino sphere at densities $\approx 10^{12}$ g/cm^3 and temperatures $T \approx 10$ MeV can be considered as a nondegenerate nucleon gas. A strong magnetic field H gives rise to a splitting $\Delta = |g_\alpha|\mu_\mathrm{N} H \equiv |g_\alpha|\omega_\mathrm{L}$ of nucleon energy levels with spin magnetic moments directed along (spin up) and opposite to (spin down) the field direction. Here μ_N denotes the nuclear magneton, $\omega_\mathrm{L} = \mu_\mathrm{N} H$ gives the Larmour frequency, and g_α is the nucleon g factor. At such conditions for neutral GT neutrino nucleon scattering, from Eqs. (1) and (2) one obtains

$$S_n \approx \sigma_{\mathrm{GT}_0} \Delta^n \Phi_n, \quad (3)$$

$$\Phi_n = [\exp\{-\delta_T\}(1+\delta_E)^2 + (-1)^n \times \exp\{\delta_T\}(1-\delta_E)^2\theta(1-\delta_E)]/\{2\cosh(\delta_T)\}, \quad (4)$$

where σ_{GT_0} denotes the neutrino–free-nucleon scattering cross section due to the neutral-current Gamow-Teller interaction component; see, e.g., [14] and references therein. Here $\delta_T = \Delta/2T$, $\delta_E = \Delta/E_\nu$, and $\cosh(x)$ is the hyperbolic cosine. The energy transfer cross section is shown in Fig. 1. Evidently, an average energy transfer, i.e., the ratio S_1/S_0, changes from positive value (i.e., exoenergetic neutrino scattering leading to acceleration) for hot nucleon gas to negative (i.e., endoenergetic neutrino stopping) for a cold system. Such a change from stopping to acceleration regimes occurs at conditions $\Phi_1 = 0$, that gives a relation $T = 0.5\Delta/[\ln\{1+\delta_E\} - \ln\{(1-\delta_E)\theta(1-\delta_E)\}]$; see also Fig. 4 and the description therein.

At a field strength $H \approx 10$ TT the level splitting $\Delta \approx$ 1–2 MeV. For neutrino energies and temperatures E_ν, $T \approx 10$ MeV, in linear approximation with δ_E and δ_T we have

$$S_1 \approx \sigma_{\mathrm{GT}_0} \Delta \delta_E (2 - E_\nu/2T), \quad (5)$$

$$S_2 \approx \sigma_{\mathrm{GT}_0} \Delta^2. \quad (6)$$

As seen from Eq. (5), at $\Delta < T, E_\nu$ the stopping and acceleration switching conditions are simplified to $T = E_\nu/4$. It is easy to understand this feature by taking into account the ratio of cross sections for scattering by spin-up S_0^{up} and spin-down S_0^{down} nucleons, $S_0^{\mathrm{up}}/S_0^{\mathrm{down}} = \exp\{\Delta/T\}\,(E_\nu - \Delta)^2/(E_\nu + \Delta)^2$, due to difference in phase space volumes and the detailed balance principle. Then for $\Delta < T$, E_ν one gets Eqs. (5) and (6) with accuracies $\mathrm{O}(\delta_T^3)$, $\mathrm{O}(\delta_T \delta_E^4)$. In this case the straggling is given by Eq. (6), i.e., a constant determined by magnetization of the SN environment. Such a property resembles the well-known Bohr limit [17] for energetic charged particles in an electron gas. As indicated in Fig. 1, the stopping-acceleration switching in the case $\Delta \approx T$, E_ν corresponds to temperatures slightly smaller than a quarter of the neutrino energy.

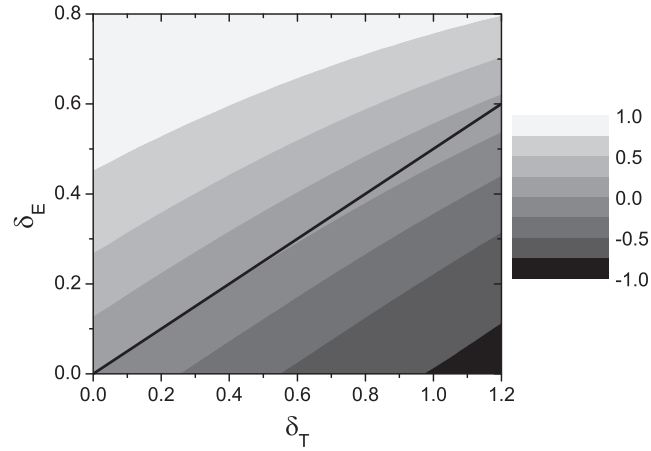

FIG. 1. Dependence of energy transfer cross sections on values δ_T and δ_E (see text) in units of $S_0\Delta$. The thick straight solid line indicates the relation $E = 4T$. The case $S_1 = 0$ corresponds to the contour including the straight line. The dark region in right bottom corner at $\delta_E < \delta_T/2$ corresponds to negative values (with minimum -1) while bright pixels in left top corner show positive average energy transfer (with maximum 1) that is related to stopping and acceleration regimes, respectively.

B. Neutrino scattering on hot atomic nuclei

As we have seen, the presence of nondegenerate nucleon energy levels gives rise to exo- and endoenergetic neutrino scattering mechanisms. To understand further the origin of such an effect and to check sensitivity to models and approximations we consider a case of neutrino scattering on hot nuclei. As an example we discuss neutrino scattering on ^{56}Fe, i.e., one of the most abundant nucleu in a SN inner mantle. A method based on a statistical formulation of the nuclear many-body problem at finite temperature, the thermal quasiparticle random-phase approximation (TQRPA) [18–20], constitutes a useful framework for accurate computing of S_n for neutrino collisions with nuclear species.

Within TQRPA the thermal strength function is expressed through eigenstates of the thermal Hamiltonian, $\mathcal{H} = H - \widetilde{H}$. Here H is the nuclear Hamiltonian and $\widetilde{H}$ is its tilde counterpart acting in an auxiliary Hilbert space [21]. The thermal Hamiltonian is diagonalized in terms of thermal multipole phonon operators:

$$\mathcal{H} = \sum_{Jk} \omega_{Jk}(T)(Q_{Jk}^\dagger Q_{Jk} - \widetilde{Q}_{Jk}^\dagger \widetilde{Q}_{Jk}). \quad (7)$$

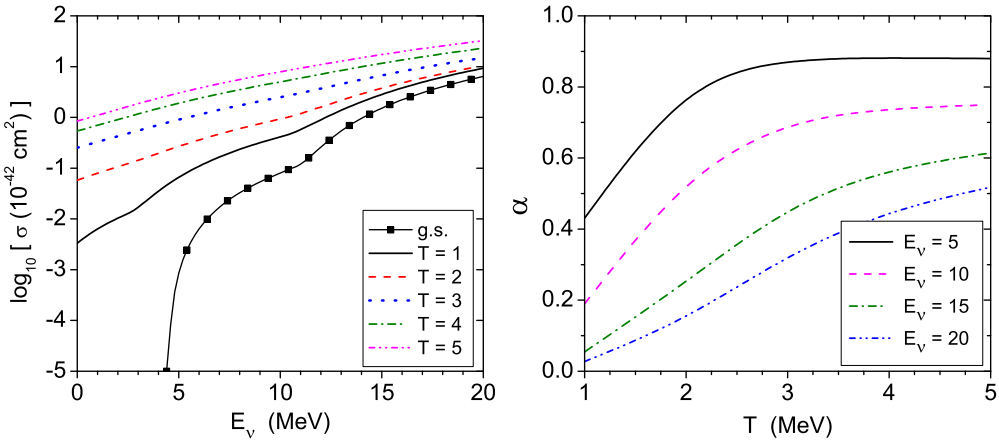

FIG. 2. Left panel: Total inelastic neutrino scattering cross sections for ^{56}Fe at different temperatures T (in MeV). Right panel: Temperature dependence of the relative fraction of exoelastically scattered neutrinos in the cross section for different energies E_ν (in MeV) of incoming neutrinos.

The vacuum of thermal phonons, $|0(T)\rangle$, describes equilibrium states of a hot nucleus, while external perturbation due to neutrino scattering leads to phonon excitations above the thermal vacuum. For GT_0 transitions induced by neutrino scattering we consider thermal phonons with $J^\pi = 1^+$. Then, the thermal strength function is expressed through matrix elements of the GT_0 operator calculated between thermal vacuum and $J^\pi = 1^+$ eigenstates of $\mathcal{H}$:

$$\Sigma_{GT_0}(E,T) = \sum_k \{\xi_k \delta(E_k - E) + \widetilde{\xi}_k \delta(E_k + E)\}, \quad (8)$$

where transition strengths are

$$\xi_k = |\langle Q_k \| GT_0 \| 0(T)\rangle|^2, \quad \widetilde{\xi}_k = |\langle \widetilde{Q}_k \| GT_0 \| 0(T)\rangle|^2. \quad (9)$$

Transitions from thermal vacuum to non-tilde phonon states describe endoenergetic processes when a nucleus gains energy from an external probe, while transitions to tilde-phonon states correspond to exoenergetic processes, when an external probe gains energy from a hot nucleus. Respective transition strengths are connected by the detailed balance relation $\widetilde{\xi}_k = e^{-\omega_k/T}\xi_k$.

By combining the TQRPA framework with the Skyrme energy density functional SkM* (see [20] and references therein), we calculate the thermal strength function for GT_0 transitions in ^{56}Fe and analyze thermal effects in neutrino scattering in terms of energy weighted integrals (1). In the left panel of Fig. 2 we show a temperature evolution of inelastic neutrino-nucleus scattering cross sections. Referring to the figure, the ground state cross section exhibits a sharp increase within the first few MeV above threshold, $E_\nu \approx 5$ MeV. For neutrino energies $E_\nu \gtrsim 10$ MeV an excitation of GT_0 resonance dominates the reaction and the increase becomes more gradual. In ^{56}Fe the GT_0 resonance is formed by superposition of neutron and proton spin-flip transitions $1f_{7/2} \to 1f_{5/2}$ [19,20]. At $T > 0$ thermal smearing of proton and neutron Fermi surfaces unblocks GT_0 transitions which are Pauli blocked at $T = 0$ and makes possible transitions from thermally occupied to low-lying orbitals. This results in an appearance of low- and negative-energy GT_0 strength. As a consequence, the ground state reaction threshold disappears and the low-energy cross section increases up to three orders of magnitude when the temperature rises from 1 to 5 MeV. Moreover, the high-energy ($E_\nu > 10$ MeV) cross section is also enhanced due to thermal effects.

To analyze the relative importance of exo- and endoenergetic neutrino scattering processes in the thermal enhancement of the cross section, we introduce the ratio

$$\alpha(E_\nu, T) = \frac{\sigma_{\rm exo}(E,T)}{\sigma(E,T)}, \quad (10)$$

where $\sigma_{\rm exo}(E,T)$ accounts for only negative-energy GT_0 transitions. In the right panel of Fig. 2 the ratio $\alpha(E_\nu, T)$ is shown as a function of temperatures at selected incoming neutrino energies E_ν. For a given neutrino energy, the ratio $\alpha(E,T)$ gradually increases with temperature, indicating a decreasing contribution of the endoenergetic scattering processes. For low-energy neutrinos ($E_\nu < 10$ MeV), the exoenergetic scattering dominates at high temperatures. However, for neutrino energies $E_\nu > 10$ MeV an excitation of the GT_0 resonance becomes possible and an exoenergetic component of the cross section appears to be comparable to or smaller than the endoenergetic one.

Let us now consider thermal effects in neutrino-nuclear energy exchange in terms of the *stopping* power S_1 and the energy straggling S_2 values. When computing $S_{1,2}$ we do not assume that $\Delta \ll T$, E_ν and apply exact Eq. (1). In fact, for GT_0 resonance Δ reaches a value $\Delta_{GT_0} \approx 10$ MeV. Evidently, for temperatures $T = 1$–5 MeV and $E_\nu \approx 10$ MeV, we get $1 < \delta_T < 5$ and $\delta_E \approx 1$. In Fig. 3 we show the ratios S_1/S_0 and S_2/S_0 computed at different temperatures as a function of incoming neutrino energy E_ν. For the *stopping* power we observe the same tendency as for neutrino scattering in a non-degenerate magnetized nucleon gas; i.e., for a given incoming neutrino energy an average energy transfer changes from negative to positive value as the temperature increases. From the discussion above it is clear that such a switching from stopping to acceleration regime occurs due to an increasing contribution of exoenergic channels from thermally excited states. For high enough temperatures the thermal population of GT_0 resonance becomes possible and its deexcitation dom-

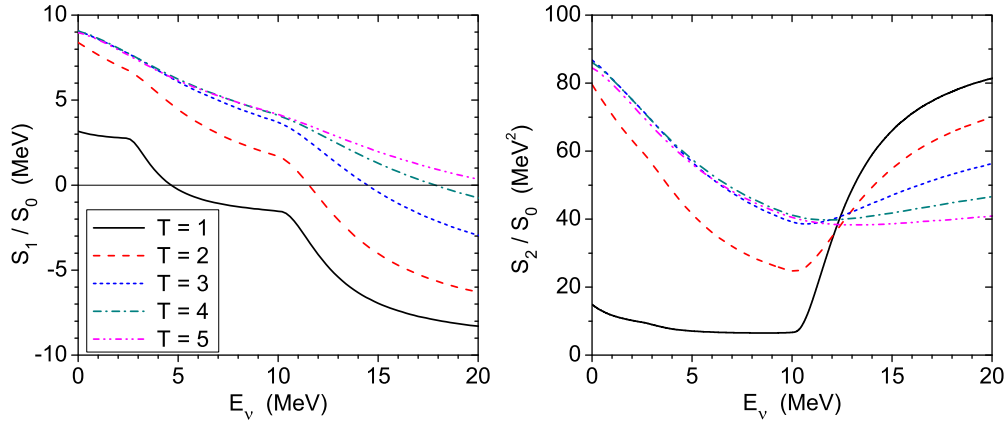

FIG. 3. Ratios S_1/S_0 (left panel) and S_2/S_0 (right panel) for inelastic neutrino scattering on ^{56}Fe at different temperatures T (in MeV) as functions of incoming neutrino energy.

inates the *stopping* power S_1 for low-energy neutrinos, making an average energy transfer $S_1/S_0 \approx 9$ MeV. Furthermore, the higher the temperature, the larger is the neutrino energy $E_\nu^{\rm cr}$ when the switch from acceleration to stopping regime occurs. For considered temperatures $T = 1$, 2, 3, 4, and 5 MeV the change occurs at energies $E_\nu^{\rm cr} \approx 4.6$, 11.6, 14.4, 18.1, and 20.5 MeV, respectively.

Figure 4 shows a relationship between incoming neutrino energies and temperatures when $S_1 = 0$, which corresponds to a sign change of an average energy transfer. As is seen, an acceleration regime is met at large temperatures $T > E_\nu/4$. This is also the case for small neutrino energies less than the endoenergetic reaction threshold. However, the scattering cross section is very small in this case. The stopping regime dominates at large neutrino energies exceeding the threshold for the endoenergetic reaction channel and $E_\nu > 4T$. For neutrino scattering on hot ^{56}Fe, at energies corresponding to an excitation of GT_0 resonance, a sign change of energy

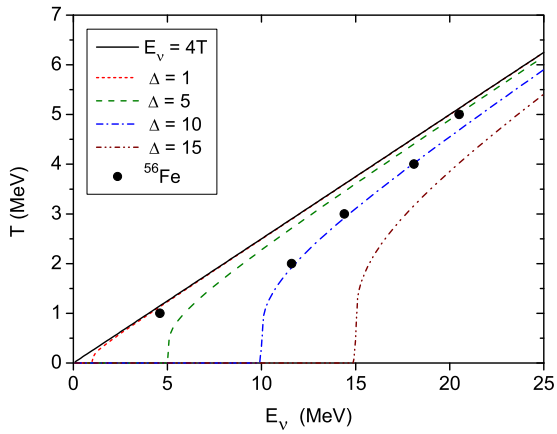

FIG. 4. The crossover between acceleration and stopping regimes in inelastic neutrino nuclear scattering. The thick straight solid line indicates the relation $E_\nu = 4T$. Dashed lines represent results for nucleon gas at several values: $\Delta = 1$, 5, 10, and 15 MeV. The dots show values for a case of ^{56}Fe at different temperatures (see the text).

transfer is well reproduced by the nucleon gas model at the value $\Delta = 10$ MeV.

As is seen in the right panel of Fig. 3 at small temperatures, the straggling changes sharply with increasing neutrino energy E_ν when it matches the GT_0 resonance threshold. At high temperatures this behavior is smeared out. Besides, the straggling increases with temperature at small neutrino energy E_ν and decreases at large E_ν exceeding the GT_0 resonance threshold. In the limit of large E_ν the straggling slightly depends on neutrino energy.

III. CONCLUSION

To summarize, we have shown that the energy transfer cross section demonstrates a change from positive to negative values with increasing neutrino energy. For a magnetized nondegenerate nucleon gas, such a crossover between acceleration and stopping regimes occurs when neutrino energy is about factor of four of gas temperature while the nucleon Larmour frequency is smaller. This switching in dynamical properties originates from the detailed balance principle and a difference of phase space volumes for neutrinos in the final channel at scattering on spin-up and spin-down nucleons. The average energy transfer, i.e., energy transfer cross section over scattering cross section, depends almost linearly on neutrino energy in such conditions. Neutrino scattering on hot atomic nuclei displays similar properties. However, the stopping regime is turned on at incoming neutrino energies slightly larger than four times the temperature because of the considerable threshold for endoenergetic reaction channels. Present calculations show noticeable values for straggling that can be enhanced due to the bunching effect.

Incorporating quantities S_n into standard transport theory allows one to consider neutrino dynamics. To evaluate the significance of energy exchange effects discussed here we analyze neutrino transport for the SN region in the vicinity of and behind the neutrino sphere when neutrino mean free path l_f is relatively large. The contribution to a change of neutrino energy dE_ν per distance dl due to the nucleon component can be written as $dE_\nu/dl|_{\rm N} = S_1\rho_{\rm N}$ with nucleon density $\rho_{\rm N}$. As is seen from Eqs. (3) and (4), at $H \approx 10$ TT the exoenergetic

reaction channel dominates for $E_\nu \approx 1$ MeV neutrinos and $dE_\nu/dl|_{\mathrm{N},E_\nu\approx 1\ \mathrm{MeV}} \approx 0.5\Delta/l_f^{(\mathrm{N})}$ with mean free path for the neutral-current Gamow-Teller interaction component $l_f^{(\mathrm{N})} = (\sigma_{\mathrm{GT}_0}\rho_{\mathrm{N}})^{-1}$. Then for densities $\rho_{\mathrm{N}} \approx 10^{12.5}$ g/cm^3 in the vicinity of the neutrino sphere one gets $dE_\nu/dl|_{\mathrm{N},E_\nu\approx 1\ \mathrm{MeV}} \approx 10^{-0.5}$ MeV/km. For MRI seed and/or shockwave front sizes of ≈1 km (see, e.g., [12] and references therein), neutrino energy changes at a value $\approx 10^{-0.5}$ MeV, comparable to $E_\nu \approx 1$ MeV considered. In the case $E_\nu \approx 10$ MeV we use Eq. (5). Then, $dE_\nu/dl|_{\mathrm{N},E_\nu\approx 10\ \mathrm{MeV}} \approx e_{\mathrm{N}}(1 - E_\nu/4T)$, where $e_{\mathrm{N}} = 2\delta_E\Delta/l_f^{(\mathrm{N})}$. At the above-mentioned conditions, i.e., densities, fields, etc., $e_{\mathrm{N}} \approx 10^{0.5}$ MeV/km and neutrino energy changes at a value $\approx 10^{0.5}$ MeV, comparable to the scale of SN neutrinos.

For neutrino scattering on iron isotope ^{56}Fe at SN values T and E_ν the energy transfer has a structure similar to that for nucleon gas; see Figs. 3 (left panel) and 4 and descriptions therein. Therefore, the corresponding change of neutrino energy per length $dE_\nu/dl|_{\mathrm{Fe}}$ is determined by $e_{\mathrm{Fe}} \approx 10\ \mathrm{MeV}/l_f^{(\mathrm{Fe})}$, where the mean free path for relevant neutrino-iron scattering reads $l_f^{(\mathrm{Fe})} = (\sigma_{\mathrm{GT}_0}\rho_{\mathrm{Fe}})^{-1}$. So, for densities $\rho_{\mathrm{Fe}} \approx 10^{11}$ g/cm^3 and the cross section shown in Fig. 2, we have $e_{\mathrm{Fe}} \approx 10^{-1}$ MeV/km. For mantle size of 100 km significant energy change can affect the neutrino spectrum.

Since neutrino energy corresponding to sign change of energy transfer depends on temperature, the neutrino spectra modification is non uniform with penetration length. Neutrinos accelerate in the SN hot inner region and lose energy in the cold mantle. Actual neutrino spectra depend on temperature profiles.

ACKNOWLEDGMENTS

The authors are indebted to an anonymous referee for careful reading of the manuscript, very useful comments, and interesting suggestions. One of us (V.N.K.) thanks the Joint Institute for Nuclear Research (Dubna) for the warm hospitality and the financial support.

[1] S. A. Colgate and R. H. White, Astrophys. J. **143**, 626 (1966).
[2] H. A. Bethe and H. A. Wilson, Astrophys. J. **295**, 14 (1985).
[3] H.-T. Janka, T. Melson, and A. Summa, Annu. Rev. Nucl. Part. Sci. **66**, 341 (2016).
[4] S. Akiyama, C. J. Wheeler, D. L. Meier, and I. Lichtenstadt, Astrophys. J. **584**, 954 (2003).
[5] J. C. Wheeler, D. L. Meier, and J. R. Wilson, Astrophys. J. **568**, 807 (2002).
[6] M. Obergaulinger, M. A. Aloy, and E. Mueller, Astron. Astrophys. **450**, 1107 (2005).
[7] S. G. Moiseenko, G. S. Bisnovatyi-Kogan, and N. V. Ardeljan, Mon. Not. R. Astron. Soc. **370**, 501 (2006).
[8] A. Burrows, L. Dessart, E. Livne, C. D. Ott, and J. Murphy, Astrophys. J. **664**, 416 (2007),
[9] T. Takiwaki, K. Kotake, and K. Sato, Astrophys. J. **691**, 1360 (2009).
[10] V. N. Kondratyev, Eur. Phys. J. A **50**, 7 (2014); Phys. Part. Nucl. **50**, 576 (2019).
[11] V. N. Kondratyev, Phys. Lett. B **782**, 167 (2018).
[12] V. N. Kondratyev and Yu. V. Korovina, JETP Lett. **102**, 131 (2015).
[13] E. P. Mazets, S. V. Golenetskii, V. N. Il'inskii, R. L. Aptekar', and Y. A. Guryan, Nature (London), **282**, 587 (1979).
[14] W. C. Haxton, Phys. Rev. Lett. **60**, 1999 (1988).
[15] S. W. Bruenn and W. C. Haxton, Astrophys. J. **376**, 678 (1991).
[16] K. Langanke, G. Martinez-Pinedo, B. Muller, H.-T. Janka, A. Marek, W. R. Hix, A. Juodagalvis, and J. M. Sampaio, Phys. Rev. Lett. **100**, 011101 (2008).
[17] N. Bohr, Mat.-Fys. Medd. K. Dan. Vidensk. Selsk. **18**, 8 (1948); *Selected Works* (Nauka, Moscow, 1970), Vol. 1 (in Russian).
[18] A. A. Dzhioev and A. I. Vdovin, Int. J. Mod. Phys. E **18**, 1535 (2009).
[19] A. A. Dzhioev, A. I. Vdovin, J. Wambach, and V. Yu. Ponomarev, Phys. Rev. C **89**, 035805 (2014).
[20] A. A. Dzhioev, A. I. Vdovin, G. Martínez-Pinedo, J. Wambach, and Ch. Stoyanov, Phys. Rev. C **94**, 015805 (2016).
[21] Y. Takahashi and H. Umezawa, Int. J. Mod. Phys. B **10**, 1755 (1996).